Lack of aggregation of molecules on ice nanoparticles

SUPPORTING INFORMATION

Andriy Pysanenko,[†] Alena Habartová,[*,‡] Pavla Svrčková,[†,¶] Jozef Lengyel,[†,¶] Viktoriya Poterya,[†] Martina Roeselová,[‡] Juraj Fedor,[*,†] and Michal Fárník[*,†]

[†]*J. Heyrovský Institute of Physical Chemistry v.v.i., Czech Academy of Sciences, Dolejškova 3, 18223 Prague 8, Czech Republic*

[‡]*Institute of Organic Chemistry and Biochemistry v.v.i., Czech Academy of Sciences, Flemingovo nám. 2, 16610 Prague 6, Czech Republic*

[¶]*Also at: Department of Physical Chemistry, University of Chemistry and Technology, Technická 5, 16628 Prague 6, Czech Republic*

E-mail: alena.habartova@marge.uochb.cas.cz; juraj.fedor@jh-inst.cas.cz; michal.farnik@jh-inst.cas.cz

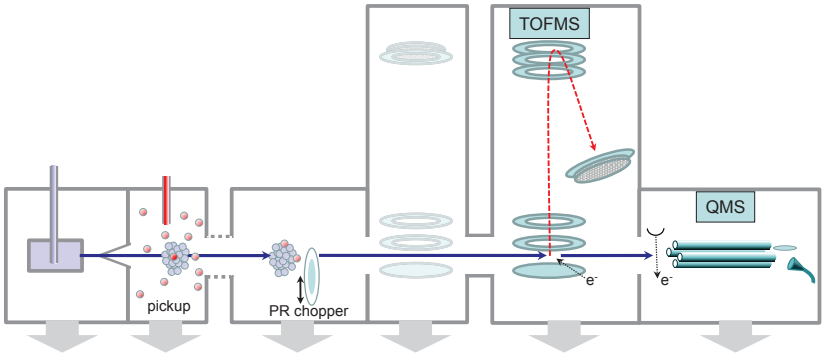

Figure 1: Scheme of the present experimental setup.

Experimental methods

Figure 1 shows the parts of universal CLUB (cluster beam) apparatus that were utilized in the present experiments. Clusters (nanoparticles) in the beam are generated via continuous supersonic expansion of either argon gas or heated water vapor through a conical nozzle. The mean cluster size $\bar{N}$ is determined from the source conditions using well-established scaling formulas[1] as described in our previous publications.[2,3] The mean size of argon clusters is

$$\bar{N} = K \cdot \left(\frac{\Gamma^*}{1000}\right)^{\zeta}, \Gamma^* = \frac{p_0[mbar] \cdot d_e[\mu m]^{0.85}}{T_0[K]^{2.2875}} \cdot K_c, \quad (1)$$

where $K = 38.4$ and $\zeta = 1.64$ were determined from the diffractive He atom scattering on large Ar_N clusters,[4] K_c =1646 is a characteristic constant of the expanding gas for Ar, and $d_e = d/\mathrm{tg}(\alpha/2)$ is the equivalent nozzle diameter.

Similarly, for water clusters

$$\bar{N} = D \cdot \left(\frac{\Gamma^*}{1000}\right)^{a}, \ \Gamma^* = \frac{\Gamma}{K_c} = \frac{n_0 \cdot d_e^q \cdot T_0^{q-3}}{K_c}, \quad (2)$$

where parameters $D = 11.6$, $a = 1.886$ and $q = 0.634$ were determined from fitting the measured size distributions of large $(H_2O)_N$ clusters.[5] The characteristic constant of the expanding gas $K_c = (r_c \cdot T_c)^{q-3}$ for water was evaluated from $r_c = 3.19$ Å and $T_c = 5684$ K.

We point out that the applicability of these formulas has been demonstrated by Buck's

Table 1: Purities and suppliers of the used chemicals

Compound	Purity	Supplier
Ar	99.998%	Messer
H_2O	distilled	Jarda Srol & Co.
HCl	anhydrous, >99%	Praxair
CH_4	99.97%	Praxair
CH_3Cl	>99.5%	Sigma-Aldrich
C_3H_7Cl	98%	Sigma-Aldrich
C_6H_6	99.8%	Lachema
C_6H_5Cl	>99.5%	Sigma-Aldrich

group in Göttingen[4,5] with the same cluster sources that are used in the present experiments. For water clusters, the reservoir temperature 420 K, stagnation pressure 4.3 bar, and nozzle with 90 μm diameter kept at 428 K lead to $\bar{N} = 430$. For argon clusters, the stagnation pressure of 7.0 bar and the 60 μm nozzle kept at 223 Kelvin leads to $\bar{N} = 330$. Both nozzles have 30 ° opening angle and 2 mm thickness.

We chose these expansion conditions to obtain argon and water clusters of approximately the same geometrical size. The geometrical cross section σ_g of the Ar_N and $(H_2O)_N$ nanoparticles is

$$\sigma_g = \pi R_N^2, R_N = R_0 N^{1/3}, R_0 = \left(\frac{3m_C}{4\pi\rho N_A}\right)^{1/3} \quad (3)$$

(N_A is Avogadro's constant). From the density ρ of solid Ar and ice we get R_0= 2.09 Å and 1.93 Å, respectively. Subsequently, the geometrical cross section is approximately the same $\sigma_g \approx 660$ Å^2 for both Ar_N and $(H_2O)_N$ of the mean sizes $\bar{N} \approx 330$ and 430, respectively. It ought to be mentioned that the geometrical cross section often includes also the radius of the molecule r_M, $\sigma_g = \pi\left(R_N + r_M\right)^2$, which is also included intrinsically in the measured cross section.[6–8] However, for the purpose of the pickup of different molecules with different radii, the geometrical cross section of the pure nanoparticles is presented here.

Table 1 shows suppliers and purities of the used chemicals.

Computational methods

All molecular dynamics calculations were performed using the GROMACS (version 4.5.4) program package.[9] The equations of motion were integrated by the leap-frog algorithm[10] with a 2 fs time step. A cut-off scheme was employed and both the Lennard-Jones and the short-range part of the Coulomb interactions were truncated to zero at 10 Å. The long-range part of the Coulomb interaction was evaluated using the smooth Particle-Mesh Ewald method[11,12] with a relative tolerance of 10^{-5}, fourth order cubic interpolation and a Fourier spacing parameter of 0.15. Temperature was controlled by the Bussi-Donadio-Parrinello (velocity rescaling with a stochastic term) thermostat[13] with a coupling time of 1 ps. All bonds were constrained by LINCS algorithm.[14] System configurations were saved at 2 ps intervals. The VMD program[15] was used for visualisation of saved trajectories to investigate structural features.

Mass spectra of adsorbed aggregates

HCl pickup: The mass spectra provide the experimental evidence for aggregation of the adsorbed molecules on Ar_N clusters. Figure 2 (a) shows the mass spectrum of pure Ar_N, $\bar{N}$= 330, clusters, and the lower panel (b) shows the spectrum of the Ar_N clusters which passed through the pickup chamber filled with HCl gas at the pressure p= 1.8×10^{-4} mbar. The upper scales label the series corresponding to the generation of HCl aggregates on Ar_N, namely the cluster ion fragments $(HCl)_m^+$ and $Ar_n\cdot(HCl)_k^+$. The spectra were measured at pickup pressures from 0.6×10^{-4} mbar to 3×10^{-4} mbar exhibiting gradual decrease of the Ar_n^+ fragment series and increase of $(HCl)_m^+$ and $Ar_n\cdot(HCl)_k^+$ series. At the highest pressure the spectrum was dominated by $(HCl)_m^+$ series. The maximum aggregate fragment size m_{max} for which the $(HCl)_m^+$ clusters were still discernible in the spectrum increased from m_{max}= 4 to 11 in the investigated pressure range, and k for the mixed fragments $Ar_n\cdot(HCl)_k^+$ increased from $k = 2$ to 6.

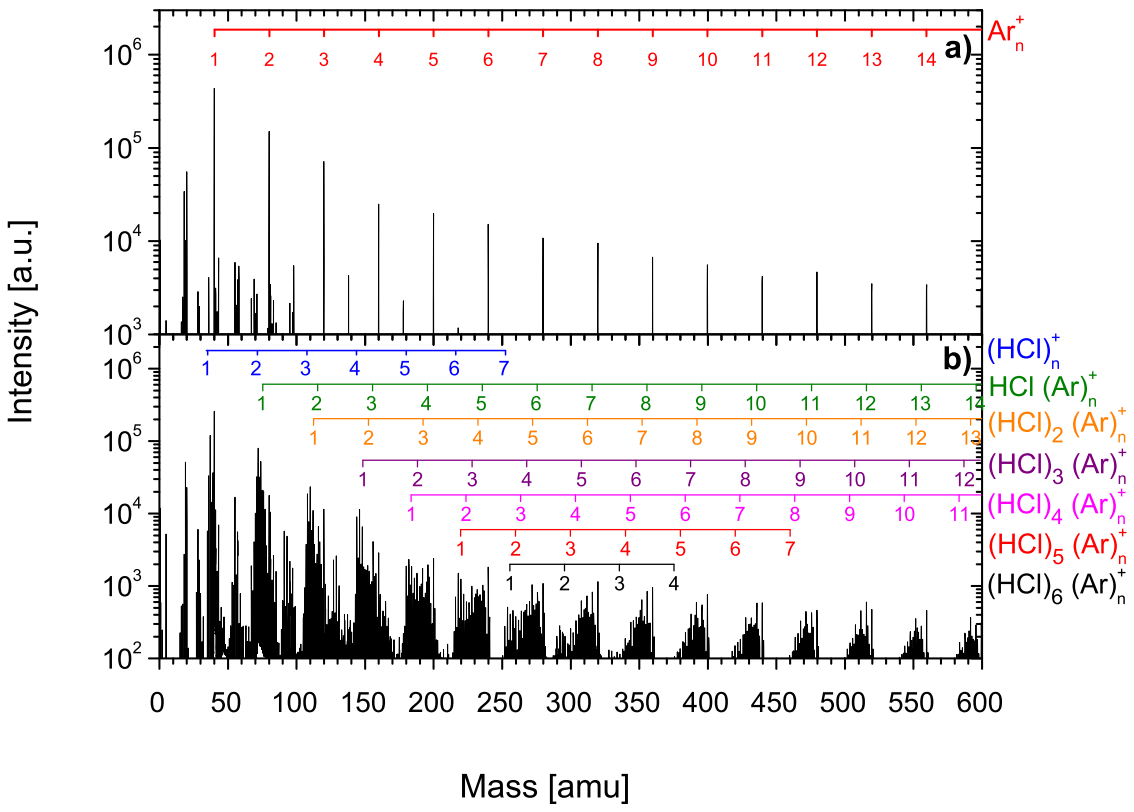

Figure 2: The mass spectrum of pure Ar_N, $\bar{N}$= 330, clusters after 70 eV electron ionization (a). The spectrum of the Ar_N clusters which passed through the pickup chamber filled with HCl gas at the pressure of 1.8×10^{-4} mbar (b). The series corresponding to the $(HCl)_m^+$ and $Ar_n\cdot(HCl)_k^+$ cluster ion fragments are labeled.

It ought to be mentioned, that due to the overlap of multiple spectra a detailed analysis was required to assign all the mass peaks unambiguously. Figure 3 shows a detail analysis of the part of the spectrum showing mass peaks corresponding to the $(HCl)_5^+$, $Ar_n\cdot(HCl)_k^+$, n= 1-4 and k= 4-1, and Ar_5^+ ion fragments. Multiple mass peaks assigned to the same cluster species occur due to the ^{35}Cl and ^{37}Cl isotopes present in the natural ratio of 3:1, and due to the presence of protonated $(HCl)_mH^+$ as well as "dehydrogenated" $(HCl)_{m-1}Cl^+$ fragments. These species appear also for the Ar containing fragments. The analysis based on the isotope ratio is outlined by the stick plot below in figure 3.

Aromatics C_6H_5Cl and C_6H_6: Extending the linear chain length of the adsorbed molecule did not have any significant influence on the clustering on Ar_N, therefore we used molecules with aromatic rings where we expected that the interaction of the ring π-electrons could

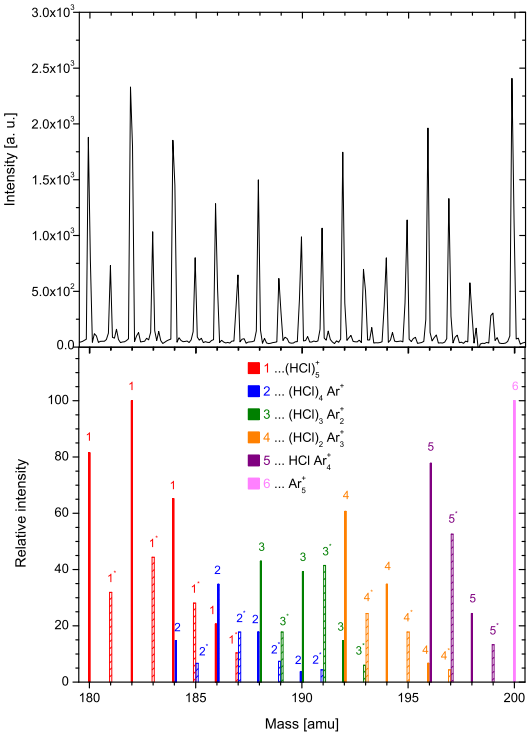

Figure 3: Detailed analysis of the mass spectrum of $Ar_N \cdot (HCl)_m$ clusters generated by pickup of HCl at the pressure of 1.8×10^{-4} mbar on Ar_N, $\bar{N}$= 330, clusters. Stick plots below show the decomposed spectra corresponding the $(HCl)_5^+$, $Ar_n \cdot (HCl)_k^+$, n= 1-4 and k= 4-1, and $Ar-5^+$ ion fragments, considering the ^{35}Cl and ^{37}Cl isotope ratio of 3:1. See text for more details.

change the coagulation behavior. Figure 4 (a) and (b) show the Ar_N cluster mass spectra after the pickup of C_6H_6 (a), and C_6H_5Cl (b). However, the spectra exhibit essentially the same clustering behavior as the linear molecules above: $(C_6H_6)_m^+$, and $Ar_n \cdot (C_6H_6)_k^+$,fragments with m_{max}= 9 and k= 1-5, for benzene at the highest pickup pressure p= 0.9×10^{-4} mbar; and $(C_6H_5Cl)_m^+$, and $Ar_n \cdot (C_6H_5Cl)_k^+$, fragments with m_{max}= 7 and k= 1-3, for chlorobenzene at the highest pickup pressure p= 0.7×10^{-4} mbar. Thus these aromatic molecules clearly coagulate to the larger clusters on Ar_N as well.

Pickup on water clusters $(H_2O)_N$: No evidence for the generation of any molecular aggregates was found in any mass spectra after the uptake of all the molecules on the ice nanoparticles $(H_2O)_N$, $\bar{N}$= 430 under analogical conditions as above. Figure 5 shows an example of the water cluster spectrum after the benzene pickup at the pickup pressure

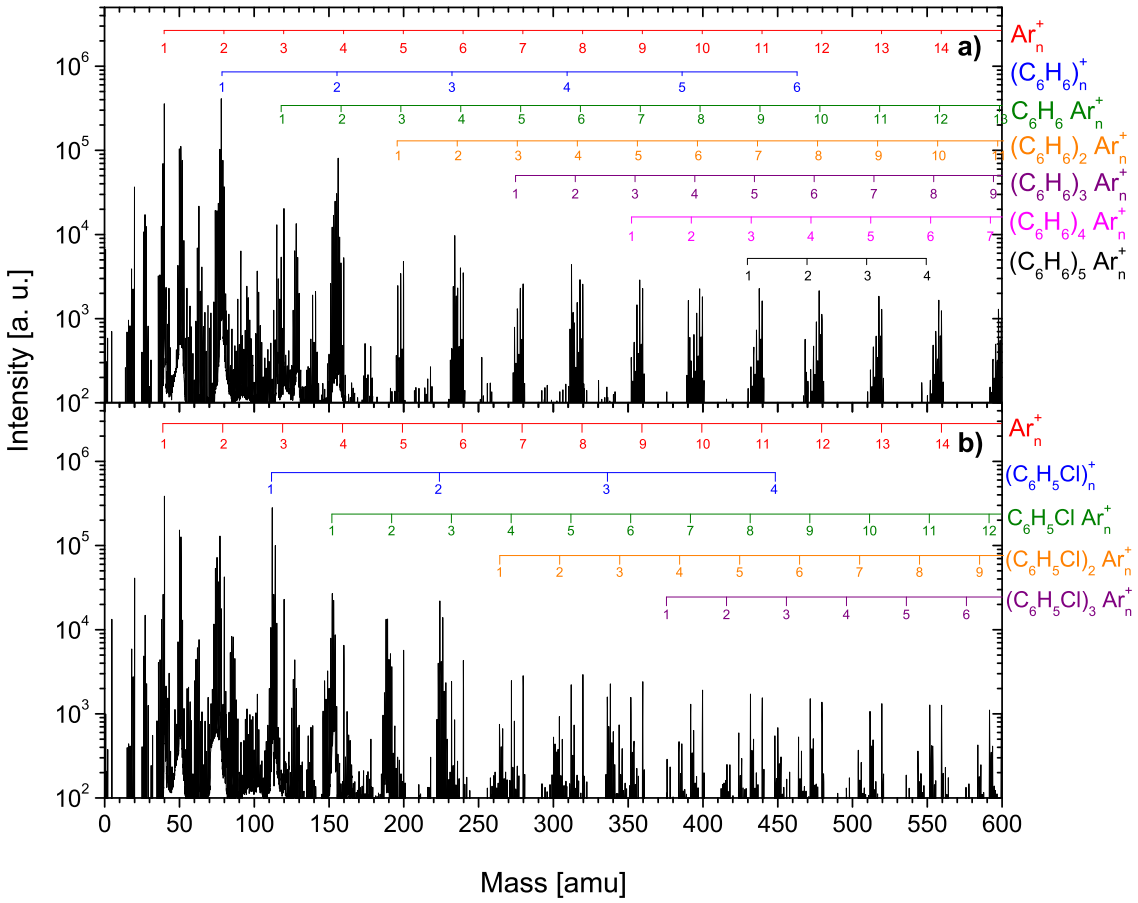

Figure 4: The mass spectrum of Ar_N, $\bar{N}$= 330, clusters after the pickup of C_6H_6 at p= 0.5×10^{-4} mbar (a), C_6H_5Cl at p= 0.4×10^{-4} mbar (b). The series corresponding to the different cluster ion fragments are labelled.

p= 0.7×10^{-4} mbar. Besides the series of protonated water cluster fragments $(H_2O)_nH^+$ there is only the mass peak corresponding to parent benzene ion $C_6H_6^+$ at 78 amu. It ought to be mentioned that the background of any C_6H_6 molecules diffused more than 1 m from the pickup chamber through the two separate differentially pumped chambers into the TOF chamber was small and carefully subtracted. Thus the C_6H_6 molecules could arrive in the TOF only with the $(H_2O)_N$ clusters. In the article, we provide further proofs that the molecules are adsorbed on the $(H_2O)_N$ nanoparticles but the mass spectra show that they do not coagulate into clusters on $(H_2O)_N$. Similar conclusions can be drawn from the mass spectra after the pickup of chlorobenzene C_6H_5Cl (figure 6), HCl and CH_3Cl (shown in the article).

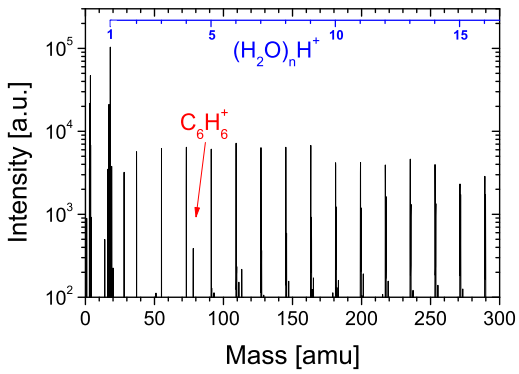

Figure 5: The mass spectrum of $(H_2O)_N$, $\bar{N}$= 430, clusters after the pickup of C_6H_6 at the pickup pressure p= 0.9×10^{-4} mbar.

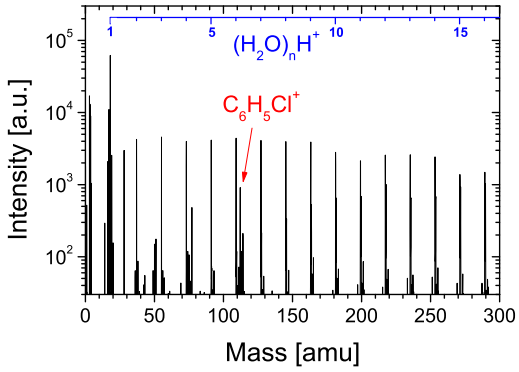

Figure 6: The mass spectrum of $(H_2O)_N$, $\bar{N}$= 430, clusters after the pickup of C_6H_5Cl at the pickup pressure p= 0.7×10^{-4} mbar.

References

(1) Hagena, O. F. Condensation in Free Jets: Comparison of Rare Gases and Metals. *Z. Phys. D* **1987**, *4*, 291 – 299.

(2) Fedor, J.; Poterya, V.; Pysanenko, A.; Fárník, M. Cluster Cross Sections from Pickup Measurements: Are the Established Methods Consistent? *J. Chem. Phys.* **2011**, *135*, 104305–1 – 10.

(3) Lengyel, J.; Kočišek, J.; Poterya, V.; Pysanenko, A.; Svrčková, P.; Fárník, M.; Zaouris, D.; Fedor, J. Uptake of Atmospheric Molecules by Ice Nanoparticles: Pickup Cross Sections. *J. Chem. Phys.* **2012**, *137*, 034304–1 – 7.

(4) Buck, U.; Krohne, R. Cluster Size Determination from Diffractive He Atom Scattering. *J. Chem. Phys.* **1996**, *105*, 5408 – 5415.

(5) Bobbert, C.; Schütte, S.; Steinbach, C.; Buck, U. Fragmentation and Reliable Size Distributions of Large Ammonia and Water Clusters. *Eur. Phys. J. D* **2002**, *19*, 183–192.

(6) Zamith, S.; Feiden, P.; Labastie, P.; L'Hermite, J.-M. Sticking Properties of Water Clusters. *Phys. Rev. Lett.* **2010**, *104*, 103401.

(7) Zamith, S.; Feiden, P.; Labastie, P.; L'Hermite, J.-M. Attachment Cross Sections of Protonated Water Clusters. *J. Chem. Phys.* **2010**, *133*, 154305.

(8) Zamith, S.; de Tournadre, G.; Labastie, P.; L'Hermite, J.-M. Attachment Cross-sections of Protonated and Deprotonated Water Clusters. *J. Chem. Phys.* **2013**, *138*, 034301.

(9) Hess, B.; Kutzner, C.; van der Spoel, D.; Lindahl, E. GROMACS 4: Algorithms for Highly Efficient, Load-Balanced, and Scalable Molecular Simulation. *Journal of Chemical Theory and Computation* **2008**, *4*, 435–447.

(10) Hockney, R.; Goel, S.; Eastwood, J. Quiet High-Resolution Computer Models of a Plasma. *Journal of Computational Physics* **1974**, *14*, 148–158.

(11) Darden, T.; York, D.; Pedersen, L. Particle Mesh Ewald: An Nlog(N) Method for Ewald Sums in Large Systems. *The Journal of Chemical Physics* **1993**, *98*, 10089–10092.

(12) Essmann, U.; Perera, L.; Berkowitz, M. L.; Darden, T.; Lee, H.; Pedersen, L. G. A Smooth Particle Mesh Ewald Method. *The Journal of Chemical Physics* **1995**, *103*, 8577–8593.

(13) Bussi, G.; Donadio, D.; Parrinello, M. COMP 8-Canonical Sampling through Velocity Rescaling. *Abstract of papers of the American Chemical Society* **2007**, *234*.

(14) Hess, B.; Bekker, H.; Berendsen, H.; Fraaije, J. LINCS: A Linear Constraint Solver for Molecular Simulations. *The Journal of Computational Chemistry* **1997**, *18*, 1463–1472.

(15) Humphrey, W.; Dalke, A.; Schulten, K. VMD: Visual molecular dynamics. *Journal of Molecular Graphics* **1996**, *14*, 33–38.